# Crystal chemistry of some Fe- and Ti-poor dumortierites

VELINDA D. ALEXANDER, DANA T. GRIFFEN, TIMOTHY J. MARTIN[1]

Department of Geology, Brigham Young University, Provo, Utah 84602

ABSTRACT

Of twelve specimens of dumortierite from various localities, we have analyzed all by electron microprobe, determined lattice parameters for all, measured optical properties for six, performed X-ray crystal-structure refinements on four, and obtained infrared absorption spectra for three. Aside from major Si and Al, the only cations detected above the ~0.02 wt% concentration level were minor Ti, Fe, Mg, and Ca. Infrared spectra confirmed the presence of similar amounts of (OH) in the three specimens checked, and we assume that (OH) is present in all twelve. From rough charge-balance considerations, based on the numbers of vacancies at the partially occupied Al(1) site, it appears that there are ~0.4 (OH) per formula unit. X-ray site refinements showed the B site to be fully occupied in all four refined structures, and there are no crystallochemically reasonable substituents for three-coordinated B. All but one specimen showed a deficiency of Si, which is supplemented by substituent Al, yielding the observed full occupancy of the Si(1) and Si(2) sites. For the twelve specimens investigated, an approximate average formula is

$$Al_{6.74}(Ti,Fe,Mg,Ca)_{0.14}(Si_{2.92}Al_{0.08})BO_{17.60}(OH)_{0.40}$$
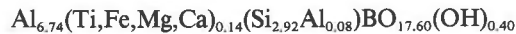
with variation expected in all subscripts, except perhaps for B.

All of our specimens were blue, pale red, or red violet and contained less Fe and Ti than brown dumortierites reported in the literature. Optical properties are linearly related to minor-element composition, such that refractive indices and birefringence increase with increasing transition-metal concentrations, but decrease as the proportion of Fe to Ti increases. Optic axial angle varies in exactly the opposite way. Color and pleochroism (blue or pale red with $E\|c$, and colorless with $E \perp c$) in these dumortierites are attributed to charge transfer among Fe^{2+}, Fe^{3+}, and Ti^{4+} replacing Al in the Al(1) face-sharing octahedral chains. It appears from the correlation between color and composition that the blue color can be attributed to Fe^{2+}-Fe^{3+} charge transfer, and the pale red to Fe^{2+}-Ti^{4+} charge transfer. The Fe:Ti ratio 1:4 separates pale-red dumortierites (poorer in Fe) from blue ones (richer in Fe).

INTRODUCTION

Dumortierite is a rather uncommon borosilicate of nonetheless widespread occurrence in pegmatitic, aplitic, and regional metamorphic rocks. It was initially identified optically over a century ago as a new mineral, but there have been few recent investigations into its crystal chemistry. Claringbull and Hey (1958) deduced the space group of dumortierite (*Pmcn*), determined unit-cell dimensions, and established the general formula as $(Al,Fe)_7BSi_3O_{18}$. They concluded that the inclusion of water in some analyses was erroneous, but our survey of later dumortierite analyses (together with infrared spectra discussed below) suggests that a small amount of H_2O is probably present. The unusually complex crystal structure was solved by Golovastikov (1965), who found that it contained isolated silicate tetrahedra, borate triangles, and three kinds of

octahedral chains, two of which involve face sharing. A structure refinement by Moore and Araki (1978) provided an elegant, detailed description of the structure and revealed that one of the chains of face-sharing octahedra is not fully occupied. We shall not reiterate their description here.

While various workers have reported chemical analyses, optical properties, or unit-cell data for individual specimens of dumortierite, a general treatment and comprehensive understanding of its crystal chemistry are lacking. As a contribution toward such a comprehensive understanding, we report here microprobe analyses and unit-cell dimensions for twelve specimens of dumortierite, along with optical properties of six of them and crystal-structure refinements of four of those six. It turns out that all of the specimens we obtained are blue, blue violet, or pale red and poorer in Fe than dumortierites of other colors reported in the literature (e.g., Black, 1973), so we are able to address crystallochemical questions concerning only a part of the known dumortierite composition range.

[1] Present address: 11677 West 62nd Avenue, Arvada, Colorado 80004.

Table 1. Unit-cell dimensions and identifying data for dumortierites included in this study

#	Locality	Source*	Peaks**	a (Å)	b (Å)	c (Å)	Volume (Å³)
1	Yuma Co., Arizona	BYU 12-5027	34P	11.789(3)	20.214(6)	4.697(2)	1119.3(4)
2	Yuma Co., Arizona	BYU 12-5026	43P	11.786(2)	20.209(4)	4.692(1)	1117.6(3)
3	(Unknown)	BYU 12-5032	48P	11.788(2)	20.195(4)	4.693(1)	1117.2(2)
4	(Unknown)	BYU 12-5028	39P	11.786(2)	20.212(4)	4.697(1)	1118.8(3)
5	Dehesa, California	BYU 12-5031	50P	11.794(2)	20.204(4)	4.694(1)	1118.5(3)
6	San Diego, California	BYU 12-5029	34P	11.781(2)	20.177(3)	4.692(1)	1115.4(2)
7	Virgin Mts., Nevada	BYU 12-5119	24S	11.798(3)	20.210(4)	4.710(2)	1123.1(4)
8	Riamfotsky, Madagascar	USNM 141247	20S	11.791(5)	20.195(8)	4.693(2)	1117.4(4)
9	Humbolt Range, Nevada	USNM 95775	45P	11.786(2)	20.208(5)	4.695(2)	1118.2(3)
10	Petaca, New Mexico	USNM 96698	42P	11.800(2)	20.222(4)	4.699(1)	1121.3(3)
11	Ambositra, Madagascar	USNM 141800	38P	11.802(2)	20.222(4)	4.695(2)	1120.6(3)
12	Dehesa, California	BYU 12-5035	33P	11.790(3)	20.199(5)	4.702(2)	1119.8(4)

* BYU = Brigham Young Univ. collections; USNM = U.S. National Museum collections.
** Number of peaks used in least squares unit cell refinement. P = powder data; S = single crystal data.

Judging from reported occurrences, however, the majority of dumortierites seem to fall into this part of the range.

EXPERIMENTAL PROCEDURES AND RESULTS

Lattice parameters

Unit-cell parameters for all twelve specimens under study were obtained with the least-squares computer refinement program of Evans et al. (1963) and are listed in Table 1, along with specimen identification information. Lattice parameters for ten of the dumortierites were determined from standard X-ray powder patterns recorded with Ni-filtered CuK_α radiation on a General Electric XRD-5 diffractometer. A goniometer scan rate of 2° 2θ/min was used, and annealed synthetic CaF_2 was employed as an internal standard. Owing to a lack of sufficient material, lattice parameters for the other two specimens were determined from single crystals. Thirty peaks, automatically centered at $+2\theta$ and -2θ on a Nicolet P3 four-circle single-crystal X-ray diffractometer, using monochromatized MoK_α radiation, were used in these two refinements. Peaks were indexed with reference to the calculated powder pattern of Borg and Smith (1969).

Microprobe analyses

Preliminary X-ray energy-dispersive analyses indicated that, of the elements detectable by that method, only Al, Si, Fe, Ti, Mg, and Ca were present at the ~0.02 wt% level or higher in any of our twelve specimens. Therefore, these six elements were determined by wavelength-dispersive electron microprobe using well-analyzed silicates as standards, with results as shown in Table 2. Data reduction was carried out by the method of Bence and Albee (1968), using the correction factors of Albee and Ray

Table 2. Chemical and optical data for dumortierites included in this study

Specimen # :	1	2	3	4	5	6	7	8	9	10	11	12
					Microprobe analyses							
SiO_2	29.92	30.33	30.66	29.85	29.99	30.59	31.65	30.66	31.07	31.12	31.79	31.02
TiO_2	1.21	1.78	2.00	1.16	1.56	1.37	0.12	1.76	0.91	1.97	0.32	1.23
Al_2O_3	61.55	61.44	61.95	60.87	61.49	61.71	60.56	59.18	61.09	60.59	60.81	59.89
Fe_2O_3*	0.54	0.09	0.09	0.54	0.06	0.10	0.44	0.59	0.16	0.52	0.38	0.13
B_2O_3*	6.08	6.12	6.18	6.04	6.09	6.14	6.12	6.02	6.11	6.15	6.14	6.05
MgO	0.05	0.11	0.10	0.05	0.10	0.10	0.84	0.05	0.12	0.14	0.53	0.10
CaO	0.02	0.02	0.02	0.02	0.02	0.02	0.01	0.02	0.02	0.01	0.02	0.02
H_2O*	0.60	0.60	0.60	0.60	0.60	0.60	0.60	0.60	0.60	0.60	0.60	0.60
Total	99.97	100.49	101.60	99.13	99.91	100.63	100.34	98.88	100.08	101.10	100.59	99.04
					Numbers of cations, based on 18(O,OH)							
Si	2.850	2.872	2.872	2.867	2.855	2.890	2.996	2.952	2.948	2.932	3.000	2.974
Ti	0.087	0.127	0.141	0.084	0.112	0.097	0.009	0.127	0.065	0.140	0.023	0.089
Al	6.912	6.858	6.841	6.892	6.901	6.872	6.757	6.717	6.832	6.729	6.766	6.768
Fe	0.039	0.006	0.006	0.039	0.004	0.007	0.031	0.043	0.011	0.037	0.027	0.009
B*	1.000	1.000	1.000	1.000	1.000	1.000	1.000	1.000	1.000	1.000	1.000	1.000
Mg	0.007	0.016	0.014	0.007	0.014	0.014	0.118	0.007	0.017	0.020	0.075	0.014
Ca	0.002	0.002	0.002	0.002	0.002	0.002	0.001	0.002	0.002	0.001	0.002	0.002
H*	0.38	0.38	0.38	0.38	0.38	0.38	0.38	0.39	0.38	0.38	0.38	0.38
					Optical properties							
α		1.676	1.675		1.673		1.671			1.675	1.669	
β	n. d.**	1.697	1.697	n. d.	1.696	n. d.	1.686	n. d.	n. d.	1.696	1.687	n. d.
γ		1.699	1.698		1.698		1.689			1.698	1.692	
$2V_x$		28(1)***	29(1)		29(1)		53(1)			34(1)	55(1)	

* See text for assumptions concerning boron and hydroxyl.
** n. d. = not determined.
*** Numbers in parentheses are standard deviations in degrees.

Table 3.   Crystal data for refined dumortierites

	#2	#7	#10	#11
Unique reflections	1465	1670	1679	1513
Unweighted R	0.074	0.029	0.078	0.045
Weighted R	0.053	0.023	0.062	0.035
Crystal size (μm)	70x90x150	180x210x220	100x120x460	140x200x360

(1970). Normalization of the twelve analyses to formulas based on 18(O + OH) resulted in the numbers of cations shown. (No implication is intended that these analyses represent the range of dumortierite composition. Indeed, analyses with higher Fe and Ti concentrations have been reported. We did not attempt to measure the trace amounts of Cu, Ni, and so forth, that have sometimes been reported for this mineral.) Note that the B_2O_3 concentration was inferred from the results of four structural-site refinements (see below), which showed full occupancy of the B site, and the lack of any crystallochemically reasonable substituent for three-coordinated B. Infrared spectra were run for three specimens (numbers 5, 10, and 11) using a Beckman IR-7 infrared spectrophotometer with 0.25 wt% sample concentration in KBr pellets, and all three showed small OH absorption bands of similar intensities. We thus assumed that all of our specimens contained similar amounts of (OH) and included 0.6 wt% H_2O in each of our microprobe analyses. (That amount of H_2O was chosen because it is consistent with the charge-balance requirements imposed by the partial occupancy of cation sites, discussed below.) To the extent that H_2O values actually vary (and we suspect that they do), the numbers of cations shown in Table 2, calculated on the basis of 18(O,OH), will be slightly in error. We would expect such errors to be small and to have little effect on the discussion to follow. Another minor source of error is the treatment of all Fe as trivalent. (We present optical evidence for the presence of some divalent Fe in the discussion.) We note that the average oxide total for our analyses is 100.15 wt%; if there are hidden systematic errors, they are either quite small, they cancel one another, or they are obscured by inaccuracy in the assumed H_2O.

Optical data

Dumortierite often occurs in bundles of parallel fibrous or acicular twinned crystals, which makes optical determinations difficult. Optical properties were measured for the six specimens for which suitable single crystals were found, and these are summarized in Table 2. Principal optical directions were determined by spindle stage techniques (Bloss, 1981), and indices of refraction were measured by standard oil-immersion methods. The computer program EXCALIBUR (Bloss, 1981) was used for determination of $2V$ from extinction-curve data, and standard deviations are given in parentheses in Table 2. All specimens were optically negative, with $c = X$, $b = Y$, and $a = Z$. Estimated errors for indices of refraction are ±0.002.

Structure refinements

Only four of our twelve specimens (numbers 2, 7, 10, and 11 in Table 1) were found to contain single crystals suitable for crystal structure refinement. X-ray intensity data were collected on a Nicolet P3 automated four-circle single-crystal diffractometer, using graphite-monochromated MoK_α radiation. Intensity scans in the range $0° < 2\theta < 65°$ were executed in the θ–2θ mode at scan rates automatically varied from 2.0° 2θ/min to 29.3° 2θ/min, depending on diffracted intensity. The intensities of three standard reflections were monitored once in every hundred reflections, and automatic recentering of the crystals and recalculation of the orientation matrices took place every 500 reflections. Lorentz-polarization corrections were applied, and the structures were refined in space group $Pmcn$ by least-squares methods using the program package SHELX-76 (Sheldrick, 1976), and starting atomic positional parameters from Golovastikov (1965), with the origin shifted to agree with that of Moore and Araki (1978). Coefficients in the expression $\Sigma\, a_i \exp[-b_i \sin^2\theta/\lambda^2 + c]$ for neutral atom scattering factors for Si, Al, B, and O were taken from Cromer and Mann (1968). Because the numbers of other atoms were very small (Table 2), no attempt was made to modify these scattering factors for observed chemistry. The sizes of the crystals and the small linear absorption coefficients (~11 cm⁻¹) made absorption corrections unnecessary.

Intensity collection and refinement data are shown in Table 3. In the final cycles of refinement we used only intensities with $I > \sigma(I)$, with weights proportional to $1/\sigma^2(F)$ applied. Observed and calculated structure amplitudes are given in Table 4.[2] The refined positional parameters (varied for all atoms) and site-occupancy factors (varied for cations only) are reported in Table 5, and anisotropic temperature factor coefficients are given in Table 6 (see footnote 2). Table 7 contains important interatomic distances, and Table 8 (see footnote 2) gives bond angles.

---

[2] To obtain copies of Tables 4, 6, and 8, order Document AM-86-303 from the Business Office, Mineralogical Society of America, 1625 I Street N.W., Suite 414, Washington, D.C. 20006. Please remit $5.00 in advance for the microfiche.

Table 5.   Refined positional parameters for four dumortierites

	#2				#7				#10				#11			
	x	y	z	k*	x	y	z	k*	x	y	z	k*	x	y	z	k*
Si(1)	0.75	0.4053(1)	0.0877(5)	1.00	0.75	0.4053(0)	0.0871(1)	1.00	0.75	0.4055(1)	0.0881(5)	1.00	0.75	0.4057(1)	0.0873(3)	0.99
Si(2)	0.5240(1)	0.3281(1)	0.5876(3)	0.99	0.5243(0)	0.3283(0)	0.5870(1)	1.00	0.5237(1)	0.3282(1)	0.5875(3)	0.99	0.5246(1)	0.3282(0)	0.5873(2)	0.98
Al(1)	0.75	0.2502(2)	0.3981(10)	0.93	0.75	0.6104(0)	0.3997(3)	0.64	0.75	0.2497(2)	0.3993(10)	0.91	0.75	0.2498(1)	0.3973(6)	0.85
Al(2)	0.6103(1)	0.4722(1)	0.5573(4)	0.98	0.6104(0)	0.4725(0)	0.5580(1)	1.00	0.6104(1)	0.4722(1)	0.5582(4)	0.98	0.6102(1)	0.4725(1)	0.5580(2)	0.98
Al(3)	0.4913(1)	0.4307(1)	0.0595(3)	0.97	0.4911(0)	0.4311(0)	0.0595(1)	1.00	0.4910(1)	0.4308(1)	0.0599(4)	0.98	0.4910(1)	0.4310(1)	0.0597(2)	0.97
Al(4)	0.3581(1)	0.2893(1)	0.0578(3)	0.99	0.3586(0)	0.2891(0)	0.0576(1)	1.00	0.3577(1)	0.2892(1)	0.0577(4)	0.99	0.3585(1)	0.2890(1)	0.0576(2)	0.99
B	0.25	0.4159(4)	0.2284(20)	1.00	0.25	0.4160(1)	0.2251(6)	1.00	0.25	0.4153(4)	0.2325(19)	0.96	0.25	0.4156(3)	0.2267(11)	1.00
O(1)	0.75	0.4537(3)	0.3788(11)		0.75	0.4540(1)	0.3771(4)		0.75	0.4532(3)	0.3791(11)		0.75	0.4539(2)	0.3765(7)	
O(2)	0.75	0.3258(3)	0.1488(11)		0.75	0.3265(1)	0.1498(4)		0.75	0.3267(3)	0.1503(12)		0.75	0.3259(2)	0.1494(7)	
O(3)	0.6390(3)	0.4242(2)	0.8967(7)		0.6394(1)	0.4243(1)	0.8963(2)		0.6387(3)	0.4249(2)	0.8964(8)		0.6397(2)	0.4241(1)	0.8953(5)	
O(4)	0.4364(3)	0.2824(2)	0.4014(7)		0.4359(1)	0.2827(1)	0.4011(2)		0.4355(3)	0.2821(2)	0.3997(8)		0.4362(2)	0.2825(1)	0.3994(5)	
O(5)	0.5496(3)	0.3933(2)	0.3972(7)		0.5500(1)	0.3943(1)	0.3963(2)		0.5491(3)	0.3933(2)	0.3969(7)		0.5504(2)	0.3933(1)	0.3956(5)	
O(6)	0.4537(3)	0.3504(2)	0.8846(7)		0.4539(1)	0.3502(1)	0.8805(2)		0.4544(3)	0.3505(2)	0.8827(8)		0.4539(2)	0.3501(1)	0.8807(4)	
O(7)	0.6396(3)	0.2868(2)	0.6479(7)		0.6385(1)	0.2870(1)	0.6477(3)		0.6387(3)	0.2868(2)	0.6484(8)		0.6397(2)	0.2867(1)	0.6478(5)	
O(8)	0.25	0.3500(3)	0.1685(12)		0.25	0.3505(1)	0.1621(4)		0.25	0.3506(3)	0.1701(13)		0.25	0.3502(2)	0.1623(7)	
O(9)	0.3507(3)	0.4482(2)	0.2553(8)		0.3511(1)	0.4479(1)	0.2548(3)		0.3511(3)	0.4486(2)	0.2553(9)		0.3511(2)	0.4480(1)	0.2540(5)	
O(10)	0.25	0.2723(3)	0.7603(11)		0.25	0.2724(1)	0.7612(4)		0.25	0.2724(3)	0.7615(12)		0.25	0.2723(2)	0.7614(7)	
O(11)	0.4663(3)	0.4881(2)	0.7505(7)		0.4464(1)	0.4881(1)	0.7499(2)		0.4661(3)	0.4881(2)	0.7512(7)		0.4661(2)	0.4881(1)	0.7503(5)	

* Corrected site occupancy factors (see text); esd's are less than or equal to 0.01 in all cases
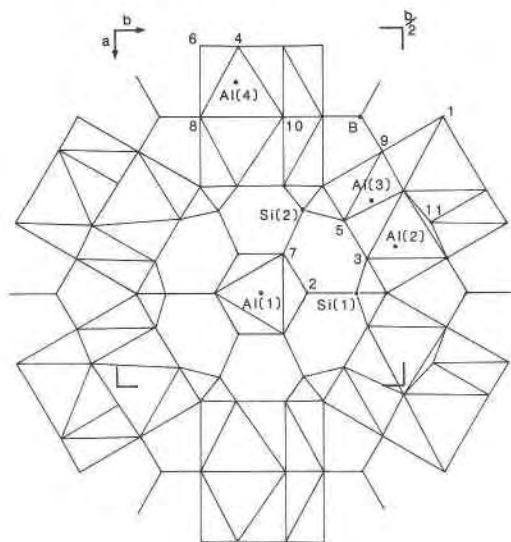
Fig. 1. A view of the dumortierite structure down **c** (after Moore and Araki, 1978). For B, Si(1), and Si(2), cation–oxygen bonds are shown. For Al(1–4), polyhedra are drawn around central cations. Numbers adjacent to polyhedral corners are oxygen designations [i.e., 8 = O(8), etc.]. See text for a brief description of the structure.

In their refinement of the dumortierite structure, Moore and Araki (1978) found that the site occupancies of Al(2), Al(3), and Al(4) converged to about 0.95, based on their assumption of full Al occupancy. In our refinements, we also found Al(2), Al(3), and Al(4) to converge to about 0.95, the B site to converge to ~0.94, and the Si(1) and Si(2) sites to converge to ~0.95. Al(1) was clearly only partially occupied in all four of our specimens, but partial occupancy of *all* cation sites seemed unlikely. As a test, we varied the site occupancies in a refinement of the structure of howlite, a calcium borosilicate (Griffen and Bailey, in prep.), and found similar cation occupancies. Because there is no reason to suspect other than full occupancy for the howlite cation sites, we interpret all of the cation sites but Al(1) in our dumortierites to be essentially fully occupied. The discrepancy evidently arises from correlation between the site occupancies and temperature-factor coefficients, and the latter are thus probably slightly low. The site occupancies shown in Table 5 are refined occupancies divided by a 0.95 empirical correction, but the standard deviations of ≤0.01 are those of the uncorrected refined site occupancies.

DISCUSSION

Crystal structure and structural chemistry

The structure of dumortierite is strongly psuedohexagonal, with **c** the pseudohexad axis. The three kinds of octahedral chains are shown in Figure 1, which is a view down **c**. The Al(1) chain is an infinite face-sharing chain parallel to [001]. The other two chains are double chains linked to one another by corner sharing, and both also extend parallel to [001]. The Al(2)-Al(3) chain is a pyroxene-like linkage made double by the inversion center at (½,½,½), so that only edges are shared between any adjacent octahedra. The Al(4) chain is also pyroxene-like, but is made double by reflection across a mirror perpendicular to [100] at *a*/4; this results in pairs of octahedra
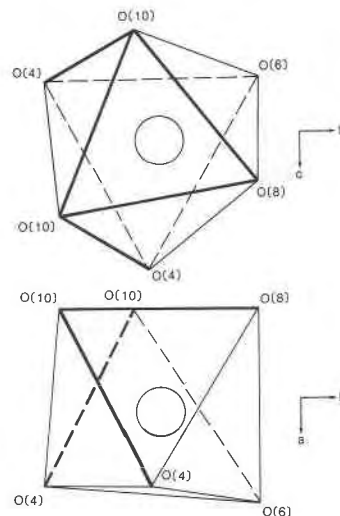

Fig. 2. Two views of the Al(4)O$_6$ octahedron, showing shared edges as heavy lines.

sharing faces across the mirror. Silicate tetrahedra link the central Al(1) chain to the surrounding octahedral chains, and borate triangles serve to strengthen the connection between one Al(4) and two Al(2)-Al(3) chains by corner sharing. Our structure refinements confirm the essential features found by Golovastikov (1965) and Moore and Araki (1978), but differ in some of the details, as discussed below.

Moore and Araki (1978) concluded, on the basis of their 0.75 site occupancy at the Al(1) site, that the Al(1) chain consists, on the average, of trimers separated by single octahedral vacancies. Had they corrected that occupancy in the same way that they corrected the apparent discrepancies in the other octahedral site occupancies, they would have obtained ~0.8, which would have led them to postulate 0.60 (OH) per formula unit instead of 0.75 (OH), and Al(1) tetramers instead of trimers. Moreover, inasmuch as they gave no chemical data, but assumed all atoms at Al(1) to be Al and all at Si(1,2) to be Si, it is not possible to assess how charge-balance considerations would have changed their (OH) estimate. As our (OH) estimates were derived from X-ray data, ignoring cationic substitutions, we consider them little more than rough estimates. It seems likely that (OH) must vary with both the numbers of octahedral vacancies and the tetravalent and divalent substituents and is therefore not a constant for dumortierite. Because the data for our four refined specimens yield about eight to nine occupied Al(1) sites out of every ten, and the amounts of potential substituents shown in Table 2 are small, we do not expect the variation to be large.

Although the mean bond lengths shown in Table 7 do not differ markedly from those given by Moore and Araki (1978), some of the trends in individual bond lengths do. Comparison of the relevant tables shows that all four of our specimens exhibit substantially larger ranges in both Si(1)–O and Si(2)–O bond lengths and smaller ranges in bond lengths about Al(1). There are no apparent corre-
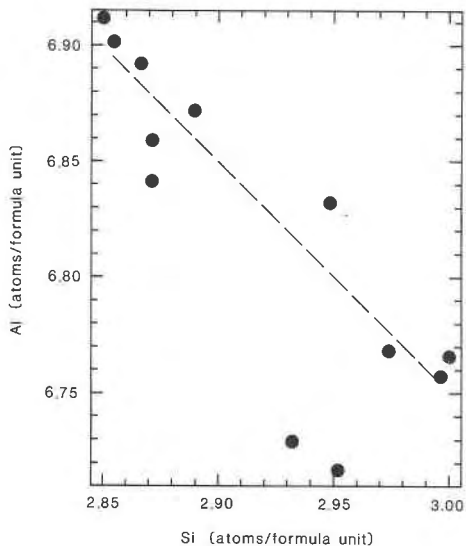
Fig. 3.   Si vs. Al, in atoms per formula unit.

Fig. 4.   Si vs. Al', where Al' is total Al minus the amount required to make up the deficiency in Si [i.e., Al' = Al − (3.00 − Si)].

lations between these bond-length ranges and the R factors, the mean bond lengths, or the equivalent isotropic temperature factors or site-occupancy factors of atoms involved in the bonds. Neither do they appear to correlate with any variations in chemical composition or with polyhedral distortions. Moreover, the ranges in bond lengths about the other cations are comparable for both studies. Although no explanation for these differences seems apparent to us, there appears to be no clear evidence that they are artifacts, either.

Calculation of bond strengths using the bond strength–bond length curves of Brown and Shannon (1973) yields results within 5% of 2.00 for all oxygen atoms but two: O(8) is over 0.20 too high, and O(10) is over 0.25 too low in all four structures.[3] Both of these atoms are bonded to Al(4) and are the corners of the shared faces in the double face-sharing chain. Moore and Araki (1978) have explained the long Al(4)–O(10) bonds as a result of the near-coplanarity of the O(10) atom and the four surrounding Al(4) atoms. Figure 2 shows an Al(4)O$_6$ octahedron, with the shared edges indicated. The average length of the five shared edges is ~2.52 Å, and that of the unshared edges is ~2.78 Å. Although the Al(1)O$_6$ octahedron has one more shared edge, its average edge length is substantially greater than that of the Al(4) site, even after correction for the larger mean bond length around Al(1). This is evidently because the shared edges at Al(1) bound shared faces on opposite sides of the octahedron, and repulsion by adjacent Al(1) atoms "stretches" the octahedron along **c.** The poor charge balance of O(8) and O(10) occurs because of the distorted shape of the Al(4) site, as well as the long Al(4)–O(10) bonds caused by mutual repulsion
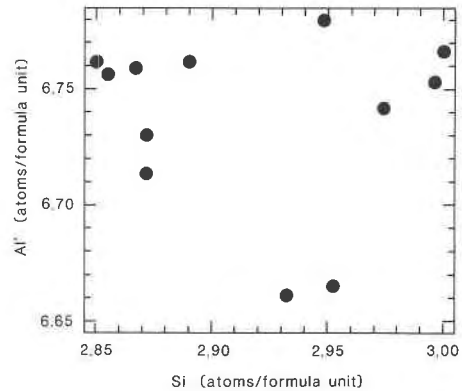
of the four coplanar Al(4) atoms noted by Moore and Araki (1978). The sharing of the five edges shown in Figure 2 causes an asymmetrical contraction of the octahedron, and the cation is displaced markedly away from the shared face; concomitantly, the shortening of the edges bounding the shared face brings O(8) close to the cation to partially compensate for the underbonding of O(10). In all four of our refinements, Al(4)–O(8) is the shortest of the six bonds in the octahedron. Moore and Araki found Al(4)–O(4) to be the shortest bond in their Al(4) site; that bond was the second shortest in three of our refinements, and the third in the other. In our four refinements, the most variable bond length about Al(4) was the one to O(6), the only oxygen not involved in a shared edge.

Chemical interrelationships

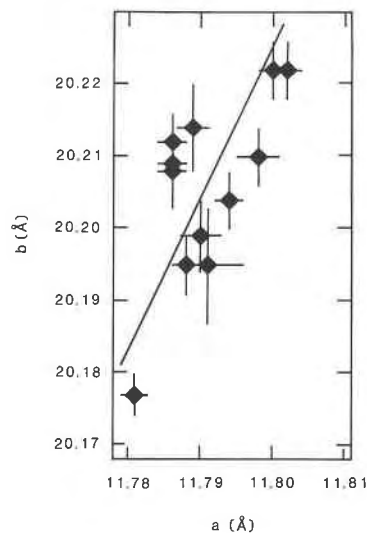The concentrations of Ti, Mg, and Fe in these dumortierites are so small that meaningful correlations among

Fig. 5.   Plot of a vs. b for twelve dumortierites.

---

[3] If partial occupancy of Al(1) is considered, the bond strengths for O(2) and O(7) are reasonable for oxygen plus appropriate (OH).
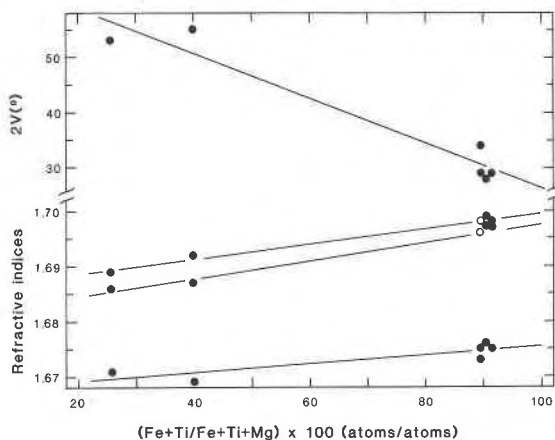
Fig. 6. Optical properties as functions of (Fe + Ti)/(Fe + Ti + Mg). Open circles represent two coincident data points.

Fig. 7. Optical properties as functions of Fe/(Fe + Ti).

them are difficult to detect. A further complication is the presence of two oxidation states of Fe, as discussed below in connection with color; however, the Fe concentration is so low that our Mössbauer spectrum of a blue dumortierite showed only background noise. The major apparent chemical relationship, seen in Figure 3, is a moderately strong antipathetic one between Si and Al. All four of our structure refinements showed the two Si sites to be essentially fully occupied, and Al is the likely substituent to make up the deficiency in Si. Figure 4 shows the Al (labeled Al') remaining after subtraction of that required to fill the Si sites, plotted against Si. Not only is there no significant correlation here, but the Al' tends to vary between quite narrow limits, except for two specimens that are about 0.10 atoms lower. This suggests that the correlation in Figure 3 results from the postulated Si-Al substitution in the Si sites, rather than from some interrelationship between ions in, say, the Si(1,2) sites and the Al(1) site. The dashed line in Figure 3 has a slope of −1, the slope required if all Si sites are filled by available Si and enough Al to total 3.0 atoms and if the remaining Al is constant; it appears to be a very reasonable slope for that data if the two low-Al analyses are ignored. Although we have no reason to suspect a problem with those two analyses, we note that a difference of less than 2% (relative) in the number of Al atoms would place them on the dashed line.

Lattice parameters

Because of the limited range of chemical compositions in these twelve dumortierites, the variations in lattice parameters are not large. Our specimens show a range of 0.021 Å in a, 0.055 Å in b, 0.018 Å in c, and 7.7 Å^3 in unit-cell volume. Figure 5 is a plot of b vs. a; the straight line was drawn by eye and has a slope of ~2. We have found no meaningful correlations between these cell dimensions and chemistry, crystal-structure variables, or other dimensional parameters. Apparently, whatever causes the increase in these cell edges affects b systemat-
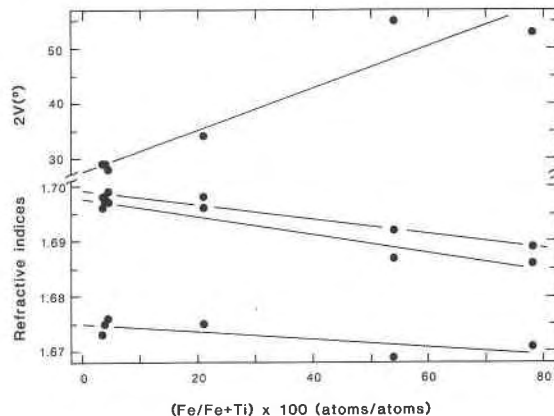
ically about twice as much as it does a, whereas a simple ionic substitution would be expected to change a and b equally, as long as the sites at which the substitution occurred were distributed equally along both axes. [Although twice as many Si(1) sites occur along b as along a (see Fig. 1), bond-length variations at this site for the four refined specimens do not vary in a way consistent with the trend in Fig. 5.]

Optical properties

Index of refraction and 2V. Figures 6 and 7 show how indices of refraction and optic axial angles are affected by changes in transition metal content. As the proportion of (Fe + Ti) relative to Mg increases (Fig. 6), indices of refraction and birefringence also increase, but 2V decreases. Exactly the opposite trends are apparent (Fig. 7) as the proportion of Fe relative to Ti increases. Unfortunately, the small range of indices of refraction and the scatter in the data, even though not large, limit the effectiveness of Figures 6 and 7 as determinative curves.

Color. The colors of the specimens under study are clearly related to the relative concentrations of Fe and Ti, as displayed by Figure 8. The transition from red to blue occurs when the Fe:Ti ratio reaches about 1:4. Observation under plane-polarized light shows that absorption is strongest when the polarization vector (**E** vector) is parallel to **c**, and that it becomes small after about 45° of microscope-stage rotation; our specimens were all colorless when the polarization vector was perpendicular to the **c** axis. This behavior is diagnostic of charge-transfer transitions (e.g., Loeffler and Burns, 1976) and indicates that
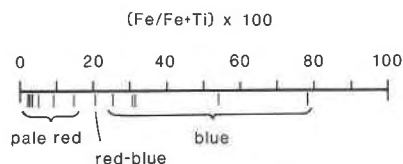

Fig. 8. The colors of twelve dumortierites as a function of Fe/(Fe + Ti).

Table 7.　Important interatomic distances for four dumortierites

Specimen # :	2	7	10	11	Specimen # :	2	7	10	11
Si(1)					**Al(3)**				
Si(1)　- O(3) x 2	1.632(4)*	1.630(1)	1.641(4)	1.628(2)	Al(3)　- O(6)	1.871(4)	1.890(1)	1.875(4)	1.889(2)
- O(2)	1.632(6)	1.620(2)	1.618(6)	1.638(4)	- O(11)	1.880(4)	1.882(1)	1.880(4)	1.879(2)
- O(1)	1.680(6)	1.684(2)	1.674(6)	1.671(4)	- O(5)	1.885(4)	1.891(1)	1.884(4)	1.887(2)
Mean	1.644	1.641	1.644	1.641	- O(3)	1.905(4)	1.916(1)	1.908(4)	1.923(2)
					- O(9)	1.928(4)	1.921(1)	1.923(4)	1.919(2)
O(3)　- O(3)	2.617(6)	2.609(2)	2.628(7)	2.607(4)	- O(11)	1.934(4)	1.930(1)	1.932(4)	1.932(2)
O(2)　- O(3) x 2	2.658(6)	2.651(2)	2.662(6)	2.657(4)	Mean	1.901	1.905	1.900	1.905
O(1)　- O(3) x 2	2.680(6)	2.682(2)	2.683(6)	2.678(4)					
O(1)　- O(2)	2.801(8)	2.791(3)	2.773(8)	2.797(5)	O(6)　- O(11)	2.856(5)	2.858(2)	2.854(5)	2.859(3)
Mean	2.682	2.678	2.682	2.679	O(6)　- O(5)	2.795(5)	2.820(2)	2.799(5)	2.813(3)
					O(6)　- O(3)	2.645(5)	2.653(2)	2.645(5)	2.657(3)
Si(2)					O(6)　- O(9)	2.898(5)	2.912(2)	2.913(5)	2.909(3)
Si(2)　- O(7)	1.621(4)	1.611(1)	1.621(4)	1.623(3)	O(11)　- O(3)	2.506(5)	2.512(2)	2.499(5)	2.518(3)
- O(5)	1.622(4)	1.622(1)	1.620(4)	1.623(2)	O(11)　- O(9)	2.849(5)	2.858(2)	2.844(5)	2.846(3)
- O(4)	1.638(4)	1.644(1)	1.653(4)	1.650(2)	O(11)　- O(11)	2.519(7)	2.530(2)	2.517(7)	2.526(4)
- O(6)	1.683(4)	1.673(1)	1.672(4)	1.671(2)	O(5)　- O(3)	2.649(5)	2.655(2)	2.657(5)	2.650(3)
Mean	1.641	1.638	1.642	1.642	O(5)　- O(9)	2.677(5)	2.677(2)	2.674(5)	2.684(3)
					O(5)　- O(11)	2.502(5)	2.499(2)	2.504(5)	2.501(3)
O(4)　- O(5)	2.609(5)	2.611(2)	2.618(5)	2.615(3)	O(3)　- O(11)	2.724(5)	2.733(2)	2.714(5)	2.736(3)
O(4)　- O(6)	2.659(5)	2.647(2)	2.667(5)	2.650(3)	O(9)　- O(11)	2.512(5)	2.512(2)	2.508(5)	2.515(3)
O(4)　- O(7)	2.661(5)	2.659(2)	2.669(5)	2.673(3)	Mean	2.678	2.685	2.677	2.685
O(5)　- O(7)	2.672(5)	2.669(2)	2.675(5)	2.677(3)					
O(5)　- O(6)	2.695(5)	2.692(2)	2.685(5)	2.694(3)	**Al(4)**				
O(6)　- O(7)	2.772(5)	2.753(2)	2.758(5)	2.768(3)	Al(4)　- O(8)	1.844(4)	1.851(1)	1.854(4)	1.848(3)
Mean	2.678	2.672	2.679	2.680	- O(6)	1.859(4)	1.867(1)	1.875(4)	1.867(2)
					- O(4)	1.863(4)	1.862(1)	1.856(4)	1.854(2)
Al(1)					- O(4)	1.868(4)	1.865(1)	1.863(4)	1.867(2)
Al(1)　- O(7) x 2	1.902(5)	1.913(2)	1.912(5)	1.901(3)	- O(10)	1.921(4)	1.925(1)	1.915(4)	1.921(3)
- O(7) x 2	1.906(5)	1.921(2)	1.912(5)	1.907(3)	- O(10)	2.019(4)	2.026(1)	2.021(4)	2.024(3)
- O(2)	1.924(7)	1.941(2)	1.949(7)	1.930(5)	Mean	1.896	1.899	1.897	1.897
- O(2)	1.934(7)	1.947(2)	1.944(7)	1.935(5)					
Mean	1.912	1.926	1.924	1.914	O(8)　- O(6)	2.745(4)	2.747(1)	2.764(5)	2.747(3)
					O(8)　- O(4)	2.809(5)	2.821(2)	2.806(5)	2.820(3)
O(7)　- O(7)	2.603(7)	2.631(3)	2.626(7)	2.605(5)	O(8)　- O(10)	2.477(7)	2.462(3)	2.487(8)	2.455(5)
O(7)　- O(7) x 2	2.778(4)	2.789(2)	2.780(4)	2.778(3)	O(8)　- O(10)	2.509(5)	2.527(2)	2.524(5)	2.519(3)
O(7)　- O(2) x 2	2.793(6)	2.805(2)	2.803(6)	2.795(4)	O(6)　- O(4)	2.795(5)	2.814(2)	2.804(5)	2.802(3)
O(7)　- O(2) x 2	2.622(6)	2.644(2)	2.644(6)	2.622(4)	O(6)　- O(4)	2.693(5)	2.696(2)	2.692(5)	2.690(3)
O(7)　- O(7)	2.603(7)	2.631(3)	2.626(7)	2.605(5)	O(6)　- O(10)	2.932(5)	2.928(2)	2.938(5)	2.930(3)
O(7)　- O(2) x 2	2.622(6)	2.644(2)	2.644(6)	2.622(4)	O(4)　- O(4)	2.687(5)	2.701(2)	2.684(5)	2.691(3)
O(7)　- O(2) x 2	2.800(6)	2.821(2)	2.818(6)	2.807(4)	O(4)　- O(10)	2.547(5)	2.547(2)	2.535(5)	2.546(3)
Mean	2.703	2.722	2.719	2.705	O(4)　- O(10)	2.547(5)	2.547(2)	2.535(5)	2.546(3)
					O(4)　- O(10)	2.776(5)	2.780(2)	2.779(5)	2.788(3)
Al(2)					O(10)　- O(10)	2.513(4)	2.523(1)	2.518(4)	2.517(2)
Al(2)　- O(11)	1.883(4)	1.886(1)	1.890(4)	1.883(2)	Mean	2.671	2.674	2.672	2.671
- O(1)	1.885(3)	1.891(1)	1.889(3)	1.896(2)					
- O(9)	1.891(4)	1.889(1)	1.880(4)	1.889(2)	**B**				
- O(3)	1.895(4)	1.899(1)	1.885(4)	1.895(2)	B　- O(8)	1.360(10)	1.356(4)	1.341(10)	1.354(6)
- O(5)	1.901(4)	1.909(1)	1.909(4)	1.909(2)	- O(9) x 2	1.360(5)	1.363(2)	1.375(5)	1.368(3)
- O(11)	1.950(4)	1.950(1)	1.956(4)	1.953(2)	Mean	1.360	1.361	1.364	1.363
Mean	1.901	1.904	1.902	1.904					
					O(8)　- O(9) x 2	2.346(6)	2.343(2)	2.348(6)	2.349(4)
O(11)　- O(1)	2.873(5)	2.872(2)	2.878(5)	2.871(3)	O(9)　- O(9)	2.373(7)	2.385(2)	2.387(7)	2.388(4)
O(11)　- O(9)	2.812(5)	2.819(2)	2.813(5)	2.817(3)	Mean	2.355	2.357	2.361	2.362
O(11)　- O(5)	2.502(5)	2.499(2)	2.503(5)	2.500(3)					
O(11)　- O(11)	2.528(5)	2.530(2)	2.538(5)	2.531(3)					
O(1)　- O(9)	2.879(5)	2.890(2)	2.884(5)	2.893(3)					
O(1)　- O(3)	2.823(5)	2.836(2)	2.822(5)	2.829(3)					
O(1)　- O(5)	2.659(4)	2.661(1)	2.663(4)	2.657(3)					
O(9)　- O(3)	2.678(5)	2.681(2)	2.659(5)	2.681(3)					
O(9)　- O(11)	2.513(5)	2.511(2)	2.508(5)	2.516(3)					
O(3)　- O(5)	2.644(5)	2.655(2)	2.652(5)	2.648(3)					
O(3)　- O(11)	2.506(5)	2.512(2)	2.499(5)	2.518(3)					
O(5)　- O(11)	2.716(5)	2.722(2)	2.721(5)	2.726(3)					
Mean	2.678	2.682	2.678	2.682					

* Numbers in parentheses are e.s.d's, and refer to the last decimal place.

the vector between sites involved in the intervalence-charge transfer lies along the direction of maximum light absorption. Figure 1 reveals that the most likely sites are the Al(1) octahedra. The Al(4) octahedral chains extend parallel to **c**, but the octahedra share ~{100} faces, so that the shortest metal-metal vector parallels **a** rather than **c**. Likewise, the Al(2)-Al(3) chains run parallel to **c**, but none of the metal-metal vectors do. On the other hand, Al(1) sites lie along **c** and are separated by only 2.35 Å across shared faces.

Careful observation of the blue specimens with the polarizing microscope shows that the blue color is sufficiently diminished in intensity by 20° or 30° of stage rotation (away from **E**‖**c**) to reveal the presence of some red transmitted light theretofore masked by the strong blue color. [Indeed, specimen no. 10, with an Fe/(Fe + Ti) ratio of

0.21 (Fig. 8) shows red-blue (purple) color in thin section with $E \| c$, and even the pale red of the low-Fe specimens has a slightly purplish cast.] This indicates that two charge transfers occur simultaneously to produce the red and blue colors; that is, the color is not caused by a single charge transfer that changes in energy as the concentrations of Fe and Ti change.

Based on Figure 8 and the above arguments, we conclude that the colors of Fe-poor dumortierites are caused by Fe^{2+}-Fe^{3+} and Fe^{2+}-Ti^{4+} charge transfer in the Al(1) chains, and we take this as prima facie evidence for the presence of two oxidation states of Fe in our specimens. Moreover, because the colors are most intense when the E vector is parallel to c and absent when oriented 90° to c, it appears that the Al(4) chains, and perhaps the Al(2)-Al(3) chains as well, do not contain sufficient concentrations of these substituents to contribute strongly to the colors.

We note that attributing the pale-red color to Fe^{2+}-Ti^{4+} charge transfer implies a broad absorption band centered around 500 nm. An absorption band of similar energy has been assigned to Fe^{2+}-Ti^{4+} charge transfer in tourmaline (Faye et al., 1974)—although Smith and Strens (1976) considered that assignment uncertain—and in fassaite (Strens et al., 1982). The implied relative energies of the proposed charge transfer absorptions (i.e., Fe^{2+}-Ti^{4+} higher than Fe^{2+}-Fe^{3+}) are correct (Loeffler and Burns, 1976).

CONCLUSIONS

The twelve dumortierites that we have investigated display only minor chemical variation. All are blue or pale red and, compared to brown dumortierites reported in the literature, are both Fe poor and Ti poor. Variations in lattice parameters are similarly small, and crystal-structure refinements of four specimens confirm previous structural work by Golovastikov (1965) and Moore and Araki (1978). Our work, based on electron-microprobe analyses, powder and single-crystal X-ray diffraction, optical microscopy, and infrared spectroscopy, leads to the following conclusions regarding the Fe- and Ti-poor end of the dumortierite compositional range:

1. Aside from elements in the idealized anhydrous chemical formula ($Al_7Si_3BO_{18}$), Ti, Fe, and Mg are present in small concentrations. All, or nearly all, specimens are deficient in Si. Al is partially replaced by other metals and partly by vacancies at the Al(1) site.

2. Water, as (OH), is present in the unit cell, but in concentrations probably lower than 0.5 (OH) per formula unit. Within narrow limits, we expect the numbers of hydroxyls to be variable.

3. The antipathetic relationship between Si and Al reflects substitution of Al for Si in the Si(1) and Si(2) sites, which are essentially fully occupied. The fairly consistent amount of Al remaining after the Si(1) and Si(2) sites are filled suggests that the number of Al(1) vacancies varies only slightly among specimens. Our data indicate that there is one Al(1) vacancy for every $9(\pm 2?)$ filled Al(1) sites.

4. Indices of refraction and optic axial angle are linearly related to minor element composition, such that (a) as (Fe + Ti)/(Fe + Ti + Mg) increases, indices of refraction and birefringence also increase, but $2V$ decreases, and (b) as Fe/(Fe + Ti) increases, the indices of refraction and birefringence decrease, but $2V$ increases.

5. The colors and pleochroism of blue, pale-red, and red-blue dumortierites are caused by Fe^{2+}-Fe^{3+} and Fe^{2+}-Ti^{4+} charge transfers occurring between metal atoms in the Al(1) sites. The Fe^{2+}-Fe^{3+} charge transfer results in absorption in the red end of the visible spectrum and leads to dumortierites of blue color if the Fe concentration is sufficiently high; the Fe^{2+}-Ti^{4+} charge transfer causes absorption in the blue end of the visible spectrum and leads to the pale-red color in dumortierites that have very low Fe concentrations along with Ti concentrations several to many times higher. Dumortierites with Fe:Ti ratios less than 1:4 are pale red, whereas those with higher Fe:Ti ratios are blue, within the compositional limits of our specimens; our dumortierite with Fe:Ti = 1:4 was purple.

REFERENCES

Albee, A.L., and Ray, L. (1970) Correction factors for electron probe microanalysis of silicates, oxides, carbonates, phosphates, and sulfates. Analytical Chemistry, 42, 1408–1414.

Bence, A.E., and Albee, A.L. (1968) Empirical correction factors for the electron microanalysis of silicates and oxides. Journal of Geology, 76, 382–403.

Black, P.M. (1973) Dumortierite from Karikari peninsula: A first record in New Zealand. Mineralogical Magazine, 39, 245.

Bloss, F.D. (1981) The spindle stage: Principles and practice. Cambridge University Press.

Borg, I.Y., and Smith, D.K. (1969) Calculated X-ray powder patterns for silicate minerals. Geological Society of America Memoir 122.

Brown, I.D., and Shannon, R.D. (1973) Empirical bond-strength–bond-length curves for oxides. Acta Crystallographica, A29, 266–282.

Claringbull, G.F., and Hey, M.H. (1958) New data for dumortierite. Mineralogical Magazine, 31, 901–907.

Cromer, D.T., and Mann, J.B. (1968) X-ray scattering factors computed from numerical Hartree-Fock wave functions. Acta Crystallographica, A24, 321–324.

Evans, H.T., Jr., Appleman, D.E., and Handwerker, D.S. (1963) The least squares refinement of crystal unit cells with powder diffraction data by an automatic computer indexing method (abs.). American Crystallographic Association Annual Meeting Program, 42–43.

Faye, G.H., Manning, P.G., Gosselin, J.R., and Tremblay, R.J. (1974) The optical absorption spectra of tourmaline: Importance of charge-transfer processes. Canadian Mineralogist, 12, 370–380.

Golovastikov, N.I. (1965) The crystal structure of dumortierite. Soviet Physics—Doklady, 10, 493–495.

Loeffler, B.M., and Burns, R.G. (1976) Shedding light on the color of gems and minerals. American Scientist, 64, 636–647.

Moore, P.B., and Araki, T. (1978) Dumortierite, $Si_3B[Al_{6.75}\square_{0.25}O_{17.25}(OH)_{0.75}]$: A detailed structure analysis. Neues Jahrbuch für Mineralogie Abhandlungen, 132, 231–241.

Sheldrick, G.M. (1976) SHELX-76: A programme for crystal structure determination. University of Cambridge.

Smith, G., and Strens, R.G.J. (1976) Intervalence-transfer absorption in some silicate, oxide and phosphate minerals. In R.G.J. Strens, Ed. The physics and chemistry of minerals and rocks, 583–612. Wiley, New York.

Strens, R.G.J., Mao, H.K., and Bell, P.M. (1982) Quantitative spectra and optics of some meteoritic and terrestrial titanian clinopyroxenes. In S.K. Saxena, Ed. Advances in physical geochemistry, 327–346. Springer-Verlag, New York.